2024 IEEE Ultrasonics, Ferroelectrics, and Frequency Control Joint Symposium (UFFC-JS) | 979-8-3503-7190-1/24/$31.00 ©2024 IEEE | DOI: 10.1109/UFFC-JS60046.2024.10793638

Characterizing Age Dependent Ultrasonic Properties of Zebrafish Embryos Using GHz Ultrasound Imaging

Daria Shkel[1], Amit Lal[1]
[1]School of Electrical and Computer Engineering,
Cornell University, Ithaca, NY
das588@cornell.edu

***Abstract*—Zebrafish are a versatile vertebrate animal model that serves science, biomedical, and the pharmaceutical industry in gaining insights into vertebrate development and helping develop drugs for diseases. This paper demonstrates the first results on imaging zebrafish embryos using GHz ultrasonic imaging using a CMOS-integrated GHz ultrasonic transmit/receive array. Zebrafish embryos are imaged on the imager to obtain their ultrasonic impedance across the embryo with 50um spatial resolution. Embryos are imaged intermittently up to 60-70 hpf (hours-post-fertilization). Gigahertz (1-2 GHz) ultrasonic pulses that are 100 nanoseconds wide penetrate through the thin chorion of the eggs into the fluid or the embryo tissue in contact with the chorion. The measurement of the complex reflection coefficients suggests that ultrasound impedance decreases over the growth period, matching the trend measured using mechanical force probes.**

Keywords—GHz ultrasound, Zebrafish, imaging, CMOS-integrated, piezoelectric transducers.

I. Introduction

Zebrafish (ZF) is a popular vertebrate model commonly used in genetic studies, pharmaceutical testing, and general understanding of vertebrate development. ZF embryos are particularly valuable due to their quick external development and optical transparency [1]. The chorion, a thin protective tissue layer around an embryo, is important for the animal's health and for indicating aquaculture quality [2]. Due to proteolytic enzymes in the Zebrafish embryo, the thickness of this lining is believed to change during development [3-5]. By characterizing how the embryo's chorion and the embryo mechanical properties change during development, one can better predict developmental changes in mammalian models at respective stages and thus potentially detect early stages of diseases and disorders. Ultrasonic imaging is a powerful tool for measuring changes in the elastic properties of materials owing to the ultrasonic impedance being proportional to the product of elasticity and density. Ultrasonic imaging also allows for non-invasive measurements, unlike techniques such as force-sensing probes. These aspects make high-frequency ultrasound imaging a potentially advantageous alternative for accurate non-invasive mechanical measurements, especially in the GHz range. Further, ultrasonic imaging can be done in the dark, without light, which may enable the study of embryo development with and without light.

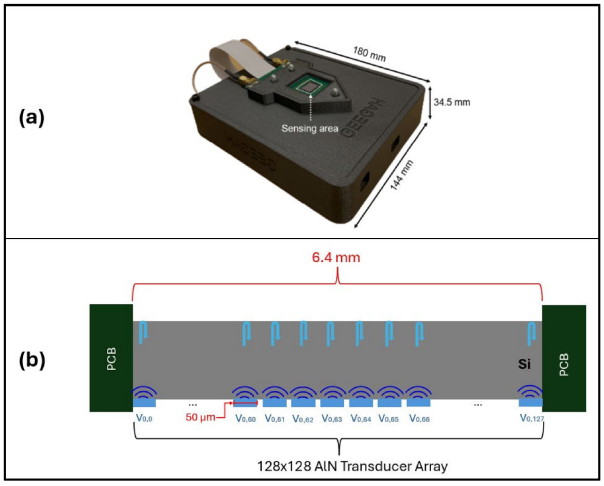

Figure 1: (a) A photo of a Geegah Imager. (b) A cross-sectional view of the ultrasound imager

II. Methods

A. GHz Ultrasonic Imager Operating Principles

All experiments in this study are facilitated using a GHz ultrasonic imager developed by Geegah Inc. It comprises a 128x128 pixel array of 50µm square and 2µm thick AlN transducers on a 130 nm integrated CMOS wafer. The CMOS circuits within each pixel are used to transmit and receive ultrasonic pulses; the pulses are RF pulses with a nominal carrier frequency of ~1.85 GHz and can be changed from 1-2 GHz. A photograph and a cross-section of the imager are shown in Fig. 1a. and Fig. 1b, respectively. The imager produces real-time images at 5-10 frames per second.

During imaging, a 100 ns transmit pulse with a user-defined carrier frequency in the 1-2 GHz range is sent from the AlN transducers through the silicon substrate to the surface of the imager, where the signal is partially absorbed by the sample and partially reflected to the transducers and receive CMOS circuitry. The reflected pulse has both a reduced amplitude and a phase shift with respect to the transmitted pulse. In-phase data (I) is collected by mixing the reflection with the in-phase and

quadrature RF carrier to obtain demodulated I and Q signals. The reflected signal is sampled at the time of expected reflection and at a time when there is no reflection to obtain high (I_{echo}) and low (I_{noecho}) voltage of the return pulse. Out of phase data (Q) is collected with the help of a local oscillator set to a 90° phase shift and again data is stored for the high (Q_{echo}) and low (Q_{noecho}) voltage of the return pulse. This is used to measure the phase shift in the reflection. All values are stored in 128x128 matrices, with each value being 12 bits, given the resolution of the ADC. The net difference between the echo and no-echo values are used as the peak-to-peak voltage values to eliminate the effect of DC biases generated by the nonlinear elements in the circuit. During imaging, the imager's baseline data, or air data without a sample, is first collected. This calibration data is required as each pixel has slight variations across the 2D array of transducers. The baseline images are later subtracted from the sample data to equalize the response and reduce effects due to variations in the array fabrication.

The ultrasonic waves at 1-2 GHz have a wavelength of 1.5 to 0.75 μm in water. The small wavelength can in principle allow very high-resolution imaging using phased arrays. However, here the lateral resolution is limited to the pixel size, which is 50 μm. The reflection coefficient from the sample at the silicon interface is $R = \frac{Z_{si}-Z_{sa}}{Z_{si}+Z_{sa}}$ where the impedance of the samples can be a complex impedance owing to the loss factor in the complex tissue.

B. Experimental Setup

In this paper, Zebrafish are observed throughout their embryonic development until hatching from ~10-60 hours post-fertilization. The embryos arrive overnight by shipping in methyl blue solution. Upon arrival, viable embryos are separated and placed into a 12-well dish with a portion of the methyl blue solution. Under ideal conditions, embryonic Zebrafish development occurs approximately 72 hours post-fertilization. At over 88% survivability, embryos exhibit normal development when kept at temperatures within a 22-32°C range [6]. To prolong experimentation time, embryos were kept at approximately 23-24 °C for slower development.

An embryo is placed under an optical microscope during experimentation, and an image is obtained for later age/development stage classification according to literature [7]. The embryo is then placed onto the ultrasonic imager after obtaining initial calibration air data. Once on the imager, any excess liquid is removed using a Kimwipe™ paper to minimize signal absorption and reflection from anything besides the embryonic tissue and air. A glass slide is placed on top, exerting a force of ~2.49 mN owing to its weight, on the embryo as an added measure to ensure the embryo has direct contact with the imager without causing excessive disturbance to the organism. The imager then obtains 20 frames worth of I and Q data. These frames are averaged in post-processing to reduce pixel noise.

For this study, data was taken approximately every 2-3 hours during the day for approximately five days until the Zebrafish were close to hatching. To minimize variables such as the effect of accumulated stress on the embryo, every experiment was done with a new specimen. After the completion of the study, all remaining fish were euthanized in a two-step process of rapid chilling in ice water and then 10 minutes in a 1:2 bleach water solution according to the Institutional Animal Care and Use Committee (IACUC) protocols and guidelines for fish within the 72 hpf development stage. The image data was then processed in Python to extract reflection coefficients and the ultrasonic impedances.

C. Data analysis

Multiple mechanical properties can be extracted from the ultrasonic signals the imager measures, which include density, elastic moduli, and viscosity. The primary parameters that were calculated and used to characterize the age of the ZF are the magnitude, phase, reflection coefficient, and acoustic impedance of the return signal. Magnitude, mathematically represented in Equation 1, is calculated by taking the squares of the net in-phase and out-of-phase voltages.

$$M = \sqrt{(I_{echo} - I_{noecho})^2 + (Q_{echo} - Q_{noecho})^2} \quad (1)$$

The magnitude (in volts) of the signal is directly proportional to the reflection coefficient through the relation $R = \frac{M_{sa}}{M_A}$, where M_{sa} is the magnitude of the return signal due to the sample, the zebrafish tissue, and M_A is the magnitude of the air return signal. The reflection coefficient and, therefore, the magnitude of the sample are inversely proportional to the acoustic impedance due to the embryo by the relation $Z_{sa} = Z_{si}\frac{1-R}{1+R}$, where Z_{sa} is the acoustic impedance of the embryo, and Z_{Si} is the acoustic impedance of the bulk silicon. The impedance of the sample is correlated with its Young's Modulus (E) and density (ρ) by the relation $Z = \sqrt{E\rho}$. The embryo's density and elasticity vary as it rotates on the imager. The tougher tissue will have higher elasticity and higher density, while the liquid around the tissue will likely have an impedance close to water.

Other studies measured the changes in the elastic modulus of the embryo chorion using piezoelectric force sensing probes. They used the probes to deform the chorion of zebrafish embryos at gastrula (5-10 hpf) and pre-hatching stages (48-72) of development until penetration of the membrane was achieved. They found that the force needed to penetrate the chorion at the gastrula and blastula (2-5 hpf) stages was 1.3 times greater than that of the pre-hatching embryos. Using force and deformation data, a biomembrane mechanics model was used to approximate the elastic modulus. They calculated a 1.66 times decrease in the elastic modulus from the early to pre-hatching stages [3]. Though the magnitude of the elastic modulus would likely be different based on methods of experimentation as well as the density of the tissue, one should also observe a decrease in the elastic modulus and, therefore, a reduction in the acoustic impedance of the chorion as the embryo develops [3].

The phase shift of the reflected pulse is also a valuable parameter to consider in this experiment. To determine the

phase of the return signal due to the US signal interaction with the sample, the inverse tangent of the ratio of the net differences between the in-phase and out-of-phase voltages is calculated as:

$$\phi = \tan^{-1}\left(\frac{I_{echo} - I_{noecho}}{Q_{echo} - Q_{noecho}}\right) \quad (2)$$

Phase imaging using the GHz ultrasonic imager is helpful in imaging objects with similar impedance but different phase shifts due to different thickness or absorption properties, akin to phase-contrast optical imaging.

III. Results and Discussion

A. Visual Comparison

The embryos generally vary in diameter from 1-1.3 mm in diameter. With a pixel size of 50μm, 20-30 pixels on a side are used to image one embryo. At the early stages of the embryo

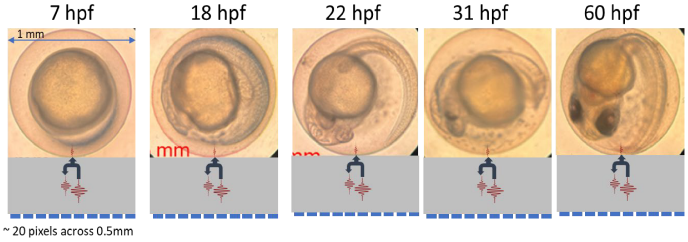

Figure 2. The embryo at different hpf (hours past fertilization) interacts with the imager differently. Optical micrographs taken using a Thorlabs microscope.

development, a fragile chorion layer surrounds the embryo with the cellular mass in the center. As the embryo grows, the cellular mass touches the chorion, and waves can penetrate the tissue. Since the embryo's position varies, the images obtained can be different, leading to different impedance measurements. Hence, the data measured here is expected to have substantial variance.

The US images of the signal magnitude, reflection coefficient, and impedance are plotted to visualize how the ultrasound signal interacts with the medium. Magnitude and phase are also calculated for the baseline air data and subtracted from the zebrafish embryo magnitude and phase signals. This is to reduce the effects of electronic noise and limit the signal coming from the embryo. Fig. 3 shows optical, magnitude, reflection coefficient, and impedance images. These average over 20 frames were used to create the result seen here.

As predicted by reflection from liquid layers, the embryo data has a lower reflection coefficient than air due to transmission into the tissue. The optical images are different embryos, but across Fig.3, the embryos whose ultrasonic properties are shown for one given time are the same. The optical and ultrasonic images show the embryo enlargement and shape change from spherical to elliptical.

B. Reflection Coefficient and Impedance Comparison to Literature

To compare how much the reflection coefficient and impedance change with age, the average value of the reflection and impedances is calculated over an 8x8 pixel region within the center of the embryo. The averaged values are plotted against the age for two different trials (Fig.4). There is a light correlation of decreasing impedance over time.

In Fig. 5b the results from the measurement of the square-root of the elastic modulus of the chorion as the zebrafish ages [3] using a mechanical force probe are plotted. Since the ultrasonic impedance of a sample is proportional to the geometric mean of the elastic modulus and the density ($Z = \sqrt{E\rho}$). The square root of the modulus can be directly compared to impedance whose plot is shown again in Figure 5a. the fractional decrease in the square root of the mechanical modulus is ~0.6%/hpf, in comparison, that for the ultrasonic impedance is similar in the 0.5-0.7%/hpf. These two similar

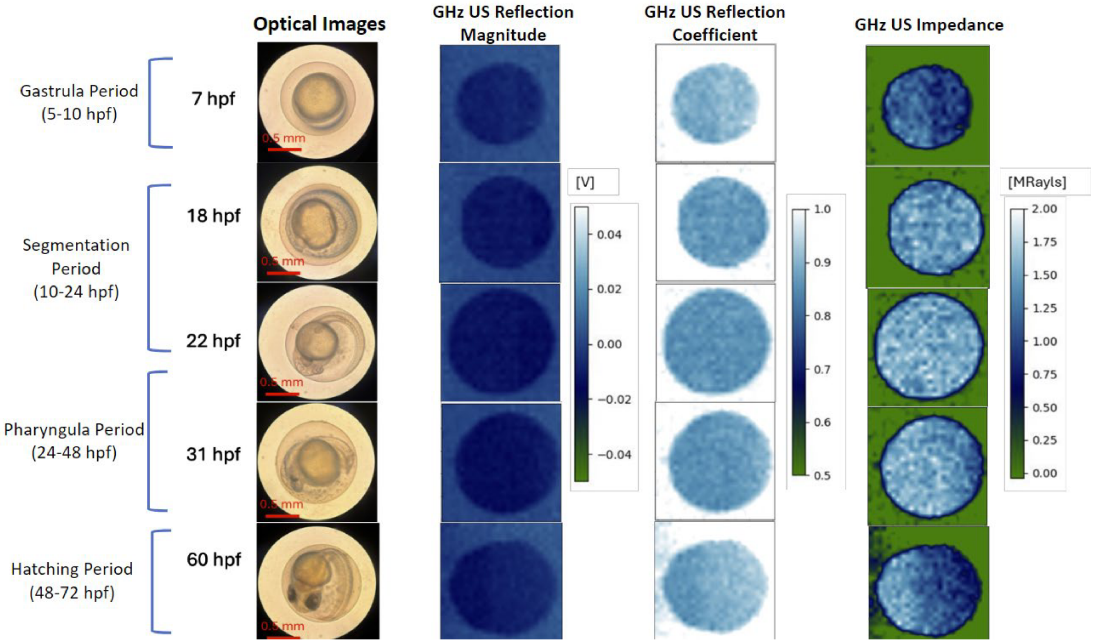

Figure 3: Zebrafish Embryos at different stages of development. Optical, US magnitude, reflection coefficient, and impedance images are shown.

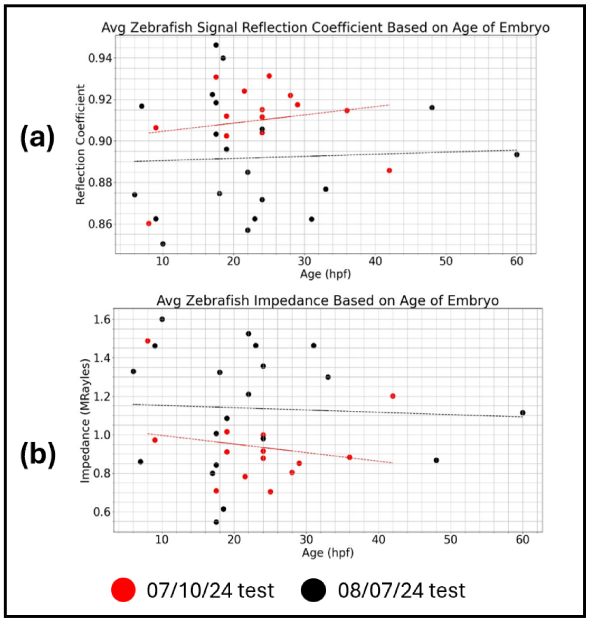

Figure 4: (a) Plot that depicts the average reflection coefficient of the return signal calculated of the return signal calculated over an 8x8 pixel area centered in the middle of the embryo for two separate trials. (b) Pot depicting the average impedance calculated over an 8x8 pixel area centered in the middle of the embryo for two separate trials over the duration of the study.

decreasing trends in elasticity must be verified with improved future experiments.

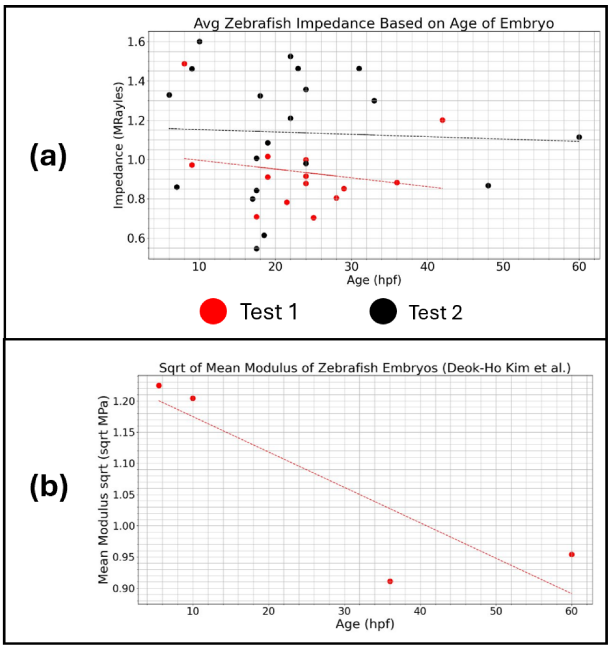

Figure 5: (a) Depicts the average impedance calculated over a 8x8 pixel area centered in the middle of the embryo for two separate trials over the duration of the study. Same as figure 3b. (b) Plot of values taken from the ultrasonic probe paper by Deok-Ho Kim et al. Plot depicts the relation between age of embryos and the square root of the mean modulus of elasticity.

A significantly improved experimental procedure is needed to reduce the variance seen in the data. As seen in Fig. 2, the embryo's position can affect the cross-section encountered by the GHz ultrasonic pulse. This is further exasperated by the fact that as a glass slide is placed on the embryo, the pressing may result in the cell-mass to come in contact with the imager. In the future, an optical microscope can be used to image the exact position of the embryo on the imager and take several images in different positions with specific orientations. A high-resolution optical image of the embryo can be superimposed on the embryo to assess the expected ultrasonic images.

IV. Conclusions and Future Outlook

This paper presents the first results of imaging zebrafish embryos using an GHz ultrasonic imager. After removing excess fluid, Zebrafish are placed on the imager to obtain the ultrasonic impedance images across an array of 128x128 50µm ultrasonic pixels. The resulting data has substantial variance due in part to the variability in the placement of the embryo tissue on the imaging surface. This variability can be reduced by correlating optical images obtained from the top side of the image at the same time as the GHz imager to determine the likely orientation of the embryo on the imager surface. Monitoring one embryo through the initial 72 hpf in a small liquid volume on the imager may further remove the embryo-to-embryo variation. This continuous imaging of a single embryo may provide further insights into mechanical property variability over the initial development hours and add further insight into vertebrate development.

ACKNOWLEDGEMENT

This work was funded under the NSF grant # 2037562. Geegah Inc. provided the imager and training on how to use it.

REFERENCES

[1] "Zebrafish: an emerging real-time model system to study Alzheimer's disease and neurospecific drug discovery | Cell Death Discovery." Accessed: Sep. 20, 2024. [Online]. Available: https://www.nature.com/articles/s41420-018-0109-7

[2] M. Pérez-Atehortúa *et al.*, "Chorion in fish: Synthesis, functions and factors associated with its malformations," *Aquac. Rep.*, vol. 30, p. 101590, Jun. 2023, doi: 10.1016/j.aqrep.2023.101590.

[3] D.-H. Kim *et al.*, "Mechanical Property Characterization of the Zebrafish Embryo Chorion," *26th Annu. Int. Conf. IEEE Eng. Med. Biol. Soc.*, vol. 2, pp. 5061–5064, 2004, doi: doi: 10.1109/IEMBS.2004.1404399.

[4] D.-H. Kim, Y. Sun, S. Yun, S. H. Lee, and B. Kim, "Investigating chorion softening of zebrafish embryos with a microrobotic force sensing system," *J Biomech*, Jun. 2005, doi: 10.1016/j.jbiomech.2004.07.014.

[5] A. F. M. Schoots, R. C. Meijer, and J. M. Denucé, "Dopaminergic regulation of hatching in fish embryos," *Dev. Biol.*, vol. 100, no. 1, pp. 59–63, doi: 10.1016/0012-1606(83)90200-2.

[6] M. E. Schnurr, Y. Yin, and G. R. Scott, "Temperature during embryonic development has persistent effects on metabolic enzymes in the muscle of zebrafish," *J. Exp. Biol.*, vol. 217, no. 8, pp. 1370–1380, Apr. 2014, doi: 10.1242/jeb.094037.

[7] C. Kimmel, W. Ballard, S. Kimmel, B. Ullmann, and T. Schilling, "Stages of embryonic development of the zebrafish," *Dev Dyn*, vol. 203, no. 3, pp. 253–310, Jul. 1995, doi: 10.1002/aja.1002030302.